



# Air Temperature

J. Mark Blonquist Jr. and Bruce Bugbee\*

## Introduction

The properties of materials and nearly all biological, chemical, and physical processes are temperature dependent. As a result, air temperature is probably the most widely measured environmental variable, and multiple sensors are available to measure it. The first thermometers were developed in the 1600s, but accurate measurement of air temperature remains a challenging task today. Instrument and method development, and error quantification, are active areas of research (Clark et al., 2013; Holden et al., 2013; Lopardo et al., 2014; Thomas and Smoot, 2013; Young et al., 2014).

Temperature indicates the relative degree of 'hotness' or 'coldness' of an object, material, or fluid. More specifically, temperature is a measure of the thermal energy of a substance. Thermal energy is associated with internal kinetic energy, or energy of motion of the atoms and molecules making up the substance. Higher temperatures correspond to higher kinetic energy (faster motion of atoms and molecules), whereas colder temperatures correspond to lower kinetic energy (slower motion of atoms and molecules). Unlike temperature of solids and liquids, air temperature is challenging to measure because air has extremely low thermal mass and thermal conductivity. This means it is difficult to get a sensor with larger thermal mass into thermal equilibrium with air. Here we review the current state of sensors and techniques for automated measurement of air temperature.

## Types of Sensors

Sensors for automated air temperature measurement include thermocouples, thermistors, platinum resistance thermometers (PRTs), integrated circuit (IC) sensors, and sonic thermometers, with thermocouples, thermistors, and PRTs being the most commonly used (Fig. 1). Each has associated advantages and disadvantages, and each will be treated separately.

## Thermocouples

A thermocouple consists of two different metals or alloys connected at the ends to form a simple electrical circuit (current loop). A temperature difference (thermal energy difference) between the two ends of the circuit produces a voltage (called an electromotive force) that is proportional to the temperature difference. This is called the Seebeck effect. The magnitude of the voltage produced depends

---

Abbreviations: IC, Integrated Circuit; PRT, Platinum Resistance Thermometer; J.M. Blonquist Jr., Apogee Instruments, Inc., 721 W. 1800 N, Logan, UT 84321; B. Bugbee, Dep. of Plants, Soils, and Climate, Utah State University, Logan, UT 84322. \*Corresponding author (bruce.bugbee@usu.edu)

doi:10.2134/agronmonogr60.2016.0012

© ASA, CSSA, and SSSA, 5585 Guilford Road, Madison, WI 53711, USA.  
*Agroclimatology: Linking Agriculture to Climate*, Agronomy Monograph 60.  
Jerry L. Hatfield, Mannava V.K. Sivakumar, John H. Prueger, editors.

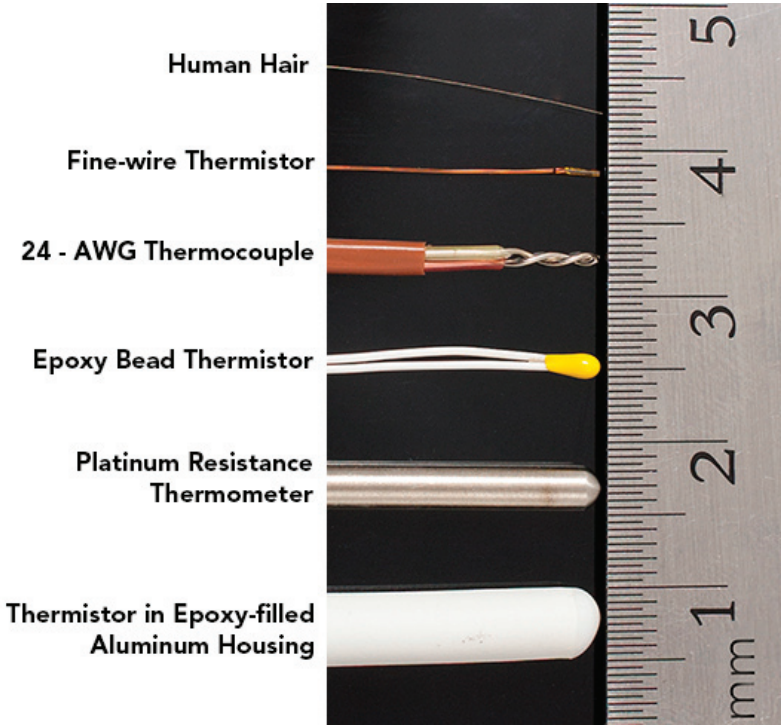


**Fig. 1. Size comparison of five temperature sensors. From top to bottom: human hair (for scale), fine wire ceramic thermistor with thin epoxy coating, 24-AWG (0.51 mm; AWG stands for American wire gauge) type-E thermocouple (multiple wire diameters are available), ceramic thermistor with epoxy bead coating, PRT in an 1/8 inch (3.18 mm) diameter stainless steel sheath, and thermistor in an epoxy-filled aluminum housing.**

on the temperature difference between the sample and reference ends, or junctions, of the circuit and the two metals used to create the circuit. The sample junction is the connection between the metals at the point where temperature is being measured, and the reference junction is the connection between the metals at the point where voltage is measured. Sometimes the sample and reference junctions are referred to as the ‘hot’ and ‘cold’ junctions, respectively, but this can be misleading because the sample junction can be hotter or colder than the reference junction. Thermocouple sample junctions are sometimes coated with epoxy for electrical isolation and waterproofing. White paint has also been used to maximize shortwave radiation reflectivity (Christian and Tracy, 1985). For air temperature measurements the epoxy coating is not essential, but it prevents corrosion and improves durability.

The voltage measured at the reference junction is nonlinearly related to the temperature difference between the junctions, and a polynomial with thermocouple-specific coefficients is typically used to convert the voltage to the temperature difference. There are multiple types of thermocouples, each with a unique combination of metals or alloys used to create the circuit. The magnitude of the voltage per degree difference (sensitivity) varies with the type of thermocouple (Table 1). Type-E thermocouples are generally considered the best option

for environmental measurements because of high sensitivity and low thermal conductivity of the wire (discussed below).

Thermocouples measure the temperature difference between the sample and reference junctions, not the actual temperature at the sample junction. The temperature at the reference junction must be known to calculate the temperature at the sample junction. One of the challenges with thermocouples is accurate measurement of the temperature at the reference junction, in addition to accurately measuring the voltage produced by the temperature difference. Some meters (e.g., dataloggers) have an internal temperature sensor (thermistor or PRT) near the reference junction (directly under the wiring panel where the lead wires of the thermocouple are connected to the meter) to measure reference temperature. The voltage change with temperature (sensitivity) of thermocouples is extremely small (Table 1), so the voltage measurement resolution and accuracy of the meter must be on the order of one micro-volt ( $\mu\text{V}$ ). Due to the small voltage output from thermocouples, electrical interference can cause errors when thermocouples are used in electrically noisy environments (e.g., near electric lights or radio equipment).

**Table 1. The four most common thermocouples used for environmental temperature measurement.**

Thermocouple	Metals or Alloys	Approximate Voltage Difference Between Junctions (Sensitivity)
Type-T	Copper (+)/Constantan (-)	40 mV $^{\circ}\text{C}^{-1}$
Type-E	Chromel (+)/Constantan (-)	60 mV $^{\circ}\text{C}^{-1}$
Type-K	Chromel (+)/Alumel (-)	40 mV $^{\circ}\text{C}^{-1}$
Type-J	Iron (+)/Constantan (-)	51 mV $^{\circ}\text{C}^{-1}$

### Thermistors

A thermistor is an electrical resistor, often ceramic or metal oxide, where resistance changes with temperature. Thermistors with a positive temperature coefficient increase in resistance with increasing temperature, whereas thermistors with a negative temperature coefficient decrease in resistance with increasing temperature. Thermistors with a negative temperature coefficient are more common. The relationship between temperature and resistance is nonlinear, and is described by a standard fitting equation, the most common being the Steinhart-Hart equation (Steinhart and Hart, 1968). The  $\beta$ -parameter equation is also used. Thermistors are typically sealed in a water-resistant or waterproof material, with epoxy and glass being common.

Thermistor resistance ( $R_T$  in  $\Omega$ ) is determined with a half-bridge measurement. The circuit is a voltage divider, with the thermistor and a bridge resistor of known and fixed resistance ( $R_B$  in  $\Omega$ ) connected in series. An excitation voltage ( $V_{EX}$  in V) is applied across the resistors (bridge resistor and thermistor in series) and voltage is measured across the bridge resistor ( $V_B$  in V). Thermistor resistance is then calculated from the voltages and  $R_B$ :

$$R_T = R_B \left( \frac{V_{EX}}{V_B} - 1 \right) \quad [1]$$

where  $V_B$  is always less than  $V_{EX}$  as a result of the voltage divider circuit. Thermistor temperature ( $T_K$ , in Kelvin) can be calculated from  $R_T$  with the Steinhart–Hart equation:

$$T_K = \frac{1}{A + B \ln(R_T) + C [\ln(R_T)]^3} \quad [2]$$

where  $A$ ,  $B$ , and  $C$  are thermistor-specific coefficients, or the  $\beta$ -parameter equation (sometimes called B-parameter):

$$T_K = \frac{\beta}{\ln\left(\frac{R_T}{R_0 e^{-\beta/T_0}}\right)} \quad [3]$$

where  $R_0$  is resistance at temperature  $T_0$  (298.15 K or 25 °C) and  $\beta$  is a thermistor-specific coefficient.

Excitation voltage is required to make the half-bridge resistance measurement, thus a small amount of power is required to measure temperature with thermistors. Current flow ( $I$ , in A) through the circuit is calculated from Ohm's Law:

$$I = \frac{V_{EX}}{R_B + R_T} \quad [4]$$

where  $R_B + R_T$  is the total resistance of the circuit. Power consumed to make the temperature measurement ( $P$ , in W) is calculated by multiplying  $I$  by  $V_{EX}$ :

$$P = IV_{EX} \quad [5]$$

where the magnitude of  $I$  and  $P$  are dependent on  $V_{EX}$ ,  $R_B$ , and  $R_T$ . Based on optimized combinations of  $R_B$  and  $V_{EX}$  for a typical thermistor ( $R_T$  versus temperature varies from thermistor to thermistor), approximate values for  $I$  and  $P$  are 0.1 mA and 0.2 mW, respectively.

Electrical current flowing through a thermistor produces heat, raising the temperature of the thermistor above air temperature. Self-heating errors for a thermistor are related to power dissipation as a result of current flow. Self-heating errors are typically minimized by intermittently powering the thermistor. They can also be reduced by decreasing current flow, which is reduced by decreasing  $V_{EX}$ . The magnitude of self-heating is calculated by dividing power input to the thermistor by the thermistor heat dissipation constant ( $W \text{ } ^\circ\text{C}^{-1}$ ). Thermistor heat dissipation constants are often measured in either still air or stirred oil. Heat dissipation is much higher for stirred oil because of higher thermal conductivity of the fluid and fluid motion. Thus, self-heating error in stirred oil is much smaller than in still air. Still air is a worst case condition for heat dissipation and self-heating error. A reasonable value for a thermistor heat dissipation constant in still air is  $1 \text{ mW } ^\circ\text{C}^{-1}$ . A reasonable value for power input to a thermistor is 0.06 mW (calculated from Eq. [5], where  $V_{EX}$  is voltage across the thermistor instead of excitation voltage). With these estimates, self-heating in still air, even with continuous excitation, is only 0.06 °C. Heat dissipation is far more efficient when air is moving, so self-heating errors should be negligible for most environmental applications.

Power consumption and self-heating can be reduced by decreasing  $V_{EX}$ . However, decreasing  $V_{EX}$  also reduces the voltage across the bridge ( $V_B$  in Eq. [1], which must be measured to determine temperature). As a result, the combination of thermistor, bridge resistor, and excitation voltage must be optimized to minimize power consumption and self-heating, and maximize voltage output and temperature measurement resolution. Typically, companies selling thermistors for air temperature measurement add the bridge resistor to the electrical circuit and suggest an optimum excitation voltage for the specific thermistor.

The bridge resistor and length of cable between the thermistor and meter (e.g., datalogger) influence the accuracy of the temperature measurement. Resistance of the bridge resistor ( $R_B$  in Eq. [1]) must be accurately determined and stable with temperature and time because it is required to calculate resistance of the thermistor. Long lengths of cable (tens to hundreds of meters) have non-negligible resistance and will contribute to total resistance when connected in series with the thermistor and bridge resistor. As an example, resistance for a common thermistor for air temperature measurement (10 k $\Omega$  at 25 °C) changes by about 30  $\Omega$  per 0.1 °C at 30 °C and 20  $\Omega$  per 0.1 °C at 40 °C. If resistance of a long cable added 20 to 30  $\Omega$ , errors would approach 0.1 °C for air temperatures in the 30 to 40 °C range. For reference, the resistance of 24-AWG (0.51-mm diam.) copper wire is about 0.053  $\Omega$  per meter. It would take about 189 m of this lead wire to produce a resistance of 20  $\Omega$  (20  $\Omega$ /0.053  $\Omega$  per meter = 378 m, but there is a wire connected to each side of the thermistor and each wire contributes to the resistance, thus 378 m is divided by two to yield 189 m). Wire resistance changes with conductor material (copper is common, but other metals and alloys are used) and diameter (smaller diameter wires have higher resistance). Thermistor resistance change with temperature is typically higher at lower temperatures, thus error from long lead wire at lower temperatures is smaller. Thermistors used with long cables can be measured in four-wire half-bridge configurations to eliminate the effects of cable resistance (this is detailed in the next section for PRTs). Reference thermistors used in laboratories for calibration of air temperature sensors are often measured in a four-wire half-bridge configuration.

### Platinum Resistance Thermometers

Like thermistors, platinum resistance thermometers (PRTs) operate by resistance change with temperature, but are made with a platinum sensing element, which is often a coiled wire or sometimes a thin film on a ceramic or plastic substrate. Thin film elements are becoming more common because they require less platinum and are lower cost. Other metals have been used in resistance temperature detectors (e.g., copper, nickel), but platinum is preferred because of high stability and wide temperature range. Platinum resistance thermometers are characterized by resistance at 0 °C, with the two most common being 100  $\Omega$  and 1000  $\Omega$ , referred to as a PT100 and PT1000, respectively.

Unlike most thermistors, the resistance of PRTs increases with increasing temperature (positive temperature coefficient), and PRTs are far more linear than thermistors over a wide temperature range. However, PRTs produce extremely small changes in resistance with temperature, which means a high resolution meter is required to make the measurement. Resistance change with temperature (sensitivity) of the PRT is quantified by the temperature coefficient of resistance ( $\alpha$ , in  $\Omega \Omega^{-1} \text{ } ^\circ\text{C}^{-1}$ ):

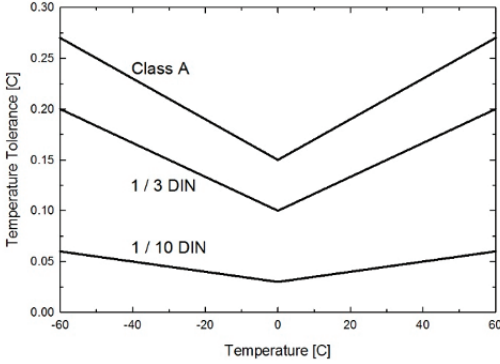


**Fig. 2. Temperature tolerance for three accuracy classifications of PRTs. Temperature tolerance specifications (y axis) are defined by International Electrotechnical Commission (2017). Some lower accuracy classes (Class B and Class C) are not shown. There is also a 1/5 DIN class, which falls between 1/3 and 1/10 DIN (DIN stands for Deutsches Institut für Normung, translating to German Institute for Standardization).**

$$\alpha = \frac{R_{100} - R_0}{100R_0} \quad [6]$$

where  $R_{100}$  is resistance at 100 °C,  $R_0$  is resistance at 0 °C, and 100 in the denominator is 100 °C. The coefficient  $\alpha$  specifies the average resistance change of the PRT from 0 to 100 °C. Common  $\alpha$  values are 0.00385 and 0.00392  $\Omega^{-1} \text{ } ^\circ\text{C}^{-1}$ , which indicate an average change in resistance of 0.385  $\Omega$  or 0.392  $\Omega$  per °C between 0 and 100 °C. These values of  $\alpha$  also indicate the resistance at 100 °C is 138.5  $\Omega$  or 139.2  $\Omega$ , assuming a resistance of 100  $\Omega$  at 0 °C (PT100).

The platinum element of a PRT is usually contained in a stainless steel sheath, making PRTs rugged and weatherproof. Multiple stainless steel sheath sizes are available (1/8-inch diam. stainless steel sheath PRT shown in Fig. 1 is small compared to most sheaths), with larger diameter and/or longer sheaths yielding slower response time of the PRT. Multiple accuracy classes of PRTs are available (Fig. 2), with cost increasing as accuracy increases.

There are three PRT wire configurations: two-wire, three-wire, and four-wire, and multiple ways (electrical circuits) to measure each configuration. In the two-wire current excitation circuit a constant excitation current ( $I_{EX}$  in A) is input to the PRT across the same wires where voltage across the PRT ( $V_{PRT}$  in V) is measured using a differential voltage measurement. Resistance of the PRT ( $R_{PRT}$   $\Omega$ ) is calculated from  $V_{PRT}/I_{EX}$  (Ohm’s Law). Measurement of  $V_{PRT}$  and input of  $I_{EX}$  must be accurate, as errors in the determination of  $R_{PRT}$  result in errors in temperature. Errors in  $V_{PRT}$  and  $I_{EX}$  can cause large temperature errors because the change in resistance with temperature (sensitivity) of PRTs is small. The half-bridge measurement described for thermistors (Eq. [1]) can be used to measure PRTs in the two-wire half-bridge circuit if a bridge resistor is included in series with the PRT. Two-wire is the simplest PRT configuration, but resistance in the lead wires connecting the PRT to the meter causes measured voltage to be higher than the voltage across the PRT, resulting in temperature errors. Sensitivity for many common PRTs is 0.385  $\Omega$  per °C ( $\alpha = 0.00385 \text{ } \Omega^{-1} \text{ } ^\circ\text{C}^{-1}$ ), resulting in errors of 1 °C for every 0.385  $\Omega$  of resistance added by lead wire. Resistance of 24-AWG (0.51-mm diam.) copper lead wire is about 0.053  $\Omega$  per meter, resulting in errors of about 1 °C for about 3.6 m of lead wire (0.385  $\Omega$ /0.053  $\Omega$  per meter = 7.2 m, but there is a wire connected to each side of the PRT and each wire contributes to the resistance, thus 7.2 m is divided by two to yield 3.6 m). Additional errors are caused by temperature-induced changes in the resistance of the lead wires, and

thermal voltages generated by dissimilar lead wire and PRT metals. These effects cause resistance changes that are not associated with the PRT. For these reasons the two-wire configuration is not common in environmental applications.

A three-wire current excitation circuit can be used to measure PRTs. Similar to the two-wire current excitation circuit,  $I_{EX}$  is applied across the PRT and  $V_{PRT}$  is measured across the PRT, but no current flows on one of the wires used for the voltage measurement, thus error from wire resistance is cut in half compared to the two-wire current excitation circuit. A three-wire half-bridge circuit can also be used to measure PRTs. In this circuit the PRT and a bridge resistor of known resistance are connected in series. An excitation voltage is applied across the resistors (bridge resistor and PRT in series) and voltage is measured across the PRT on two different wires, each connected to the same end of the PRT. Each voltage measurement uses a single-ended measurement. This accounts for lead wire resistance by assuming the resistance of the two wires over which the voltage measurements are made is the same. The impact of lead wire resistance is eliminated if lead wire resistances are indeed equal, but the challenge is matching of the wires. Error in the temperature measurement results if wires are not the exact same length or small resistance differences between lead wires are present. Measurements with PRTs with three-wire configuration are more common than those with PRTs with two-wire configuration, but air temperature measurements with PRTs are typically made with PRTs with four-wire configuration.

There are three ways to measure PRTs with four-wire configuration. In the four-wire current excitation circuit  $I_{EX}$  is applied across the PRT with two of the wires,  $V_{PRT}$  is measured across the other two wires, and  $R_{PRT}$  is calculated from  $V_{PRT}/I_{EX}$  (Ohm's Law). This requires a one differential voltage measurement. Current doesn't flow in the wires where voltage is measured, so resistance of the lead wires does not influence the measurement. In the four-wire half-bridge circuit the PRT and a bridge resistor of known and fixed resistance ( $R_B$ , in  $\Omega$ ) are connected in series. An excitation voltage ( $V_{EX}$ , in V) is applied across the resistors (bridge resistor and PRT in series) and voltages are measured across the bridge resistor ( $V_{B'}$ , in V) and PRT ( $V_{PRT'}$ , in V). Resistance from the PRT ( $R_{PRT'}$ , in  $\Omega$ ) is then calculated from the voltage measurements and  $R_B$ :

$$R_{PRT} = R_B \frac{V_{PRT}}{V_B} \quad [7]$$

where the ratio of voltages ( $V_{PRT}/V_B$ ) is equal to the ratio of resistances ( $R_{PRT}/R_B$ ). The four-wire half-bridge circuit accounts for resistance of the lead wires, like the four-wire current excitation circuit. These two circuits yield the highest accuracy temperature measurements with PRTs, but the four-wire half-bridge circuit requires two differential voltage measurements, whereas the four-wire current excitation circuit only requires one. A four-wire full-bridge configuration is also an option. It only requires one differential voltage measurement, but isn't as accurate as the four-wire current excitation and half-bridge circuits unless the two bridge resistors required for the full-bridge circuit are perfectly matched.

As with thermistors, resistance of bridge resistors must be accurately determined and stable with temperature and time. Unlike most thermistors, resistance of PRTs is relatively small (often 100  $\Omega$  or 1000  $\Omega$  at 0 °C) and resistance change with temperature is very small (as described above,  $\alpha$  for a PRT indicates the

average resistance change per degree °C between 0 and 100 °C; values of 0.385 and 0.392 Ω per °C are common). Thus, errors in bridge resistance, changes in bridge resistance, or resistance added by lead wires, on the order of small fractions of an Ohm, can have large impacts on temperature measurements. Also like thermistors, PRTs are subject to self-heating errors because electrical current is flowing through the PRT. Self-heating is minimized by minimizing the excitation current or voltage.

Temperature is typically related to  $R_{\text{PRT}}$  with the Callendar–Van Dusen Equation (Callendar, 1887; Van Dusen, 1925). The most common solutions to the Callendar–Van Dusen Equation separate the temperature scale into two parts, with 0 °C being the dividing line. When  $R_{\text{PRT}}/R_0$  is less than one (temperature is below 0 °C), where  $R_0$  is the resistance of the PRT at 0 °C, then PRT temperature ( $T_{\text{PRT}}$  in °C) equals:

$$T_{\text{PRT}} = gK^4 + hK^3 + iK^2 + jK \quad [8]$$

where  $K = (R_{\text{PRT}}/R_0) - 1$  and  $g, h, i,$  and  $j$  are PRT-specific coefficients (coefficients vary with  $\alpha$ ). When  $R_{\text{PRT}}/R_0$  is greater than or equal to 1 (temperature is above 0 °C), then  $T_{\text{PRT}}$  equals:

$$T_{\text{PRT}} = \frac{\sqrt{d(R_{\text{PRT}}/R_0) + e} - a}{f} \quad [9]$$

where  $a, d, e,$  and  $f$  are PRT-specific coefficients. Different equations for conversion of  $R_{\text{PRT}}$  to temperature have also been used. Many datalogger manufacturers have preprogrammed instructions for PRTs, which use the equations above or similar to calculate temperature from  $R_{\text{PRT}}$ . The only required input is  $\alpha$  for the PRT (to determine coefficients).

As with thermistors, PRTs require power because excitation voltage is input to determine resistance. Power requirements for PRTs are small, with 0.4 mW being a typical value. Self-heating of PRTs is present, and dependent on the voltage across the PRT. This is typically much smaller than that for a thermistor, thus self-heating of PRTs is much less than the PRT temperature tolerance (Fig. 2) and can be considered negligible. Companies selling PRTs for use as air temperature sensors typically add the necessary resistors for the different configurations and suggest an optimum excitation voltage to minimize self-heating and maximize temperature measurement resolution.

### Advantages and Disadvantages of Thermocouples, Thermistors, and Platinum Resistance Thermometers

Changes in signal (voltage, resistance) from a temperature sensor caused by changes in air temperature must be measurable, repeatable, and stable. Thermocouples, thermistors, and PRTs all require a meter (e.g., datalogger) to measure the electrical signal and convert it to temperature. This means several of the advantages and disadvantages depend on the data acquisition device. Dataloggers are desirable for environmental monitoring, where automated data collection of high frequency and/or long-term data sets are often required. The advantages and disadvantages of thermocouples, thermistors, and PRTs are summarized (Table 2). The advantages and disadvantages of PRTs are similar to or the same as those for

**Table 2. Advantages and disadvantages of thermocouples, thermistors, and platinum resistance thermometers (PRTs) when used for air temperature sensors.**

Sensor Type	Advantages	Disadvantages
Thermocouple	Does not require excitation voltage	Requires accurate reference temperature measurement
	No self-heating	Small signal change per °C change
	Multiple sensors can be made from one roll of wire	Requires differential channel on datalogger
	No compensation for long lead wires is required	Expensive wire; variability in wire from batch to batch
Thermistor	Reference temperature not required	Requires excitation voltage
	Large signal change per °C change	Self-heating error from continuously applied excitation voltage
	Only requires single-ended channel on datalogger	Can drift over time if not enclosed in water proof material
	Inexpensive wire	Long lead wires increase resistance
PRT	Reference temperature not required	Requires excitation voltage
	Inexpensive wire	Self-heating error from continuously applied excitation voltage
		Small signal change per °C change
		Requires at least one differential channel on datalogger
	Long lead wires must be compensated for with a four-wire configuration	

thermistors, except that the resistance change with temperature (sensitivity) of PRTs is much smaller and more difficult to measure, PRTs typically require at least one differential channel on a datalogger, and PRTs typically have slower response time because the housing is often much larger than that for thermistors (Fig. 1).

Some of the advantages and disadvantages depend on the circumstances of the specific measurement and application. For example, the power requirement of thermistors and PRTs is extremely small. As stated above, typical current draw for a thermistor is approximately 0.1 mA, but many dataloggers can source several mA. A common datalogger used in environmental monitoring (Campbell Scientific model CR1000) can source 25 mA. Based on this specification, this specific datalogger could accommodate 250 thermistors (or PRTs) if there were enough measurement channels available.

The reference temperature required for thermocouples is available on thermocouple-specific meters and on many dataloggers. Accurate reference temperature measurements are then dependent on the accuracy of the reference sensor. This is a thermistor or PRT. Periodic recalibration of the meter or datalogger is recommended to ensure the internal temperature sensor is accurate. Also, the datalogger wiring panel (where the thermocouples are connected) must be maintained isothermal. This is best accomplished by installing the datalogger in an insulated, weatherproof box that shields it from solar radiation.

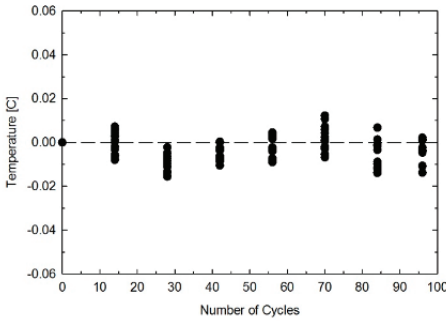


**Fig. 3. Stability of twelve replicate thermistors (Measurement Specialties model 10K3A11A) in a thermal cycling chamber. Cycles were -20 to 60 °C, with a vapor pressure range of 0.5 to 12 kPa (condensing humidity). Thermistor stability was periodically checked by removing the thermistors and measuring temperature in a slush bath (assumed to be 0 °C). The small down and up trend of the data are due to slight differences in the slush bath from one verification to the next.**

The small output signal of thermocouples and PRTs relative to the large output signal of thermistors is only a disadvantage when a low-resolution datalogger is used. Some dataloggers have adequate resolution to make accurate thermocouple and PRT measurements, but the requirement of a differential channel is always a disadvantage. This means twice as many thermistors can be connected to the same number of datalogger channels (or four times the number of thermistors if PRTs are measured in the four-wire half-bridge configuration).

Nonlinearity is typically listed as a disadvantage of thermistors (e.g., Hubbard and Hollinger, 2005), but as long as the nonlinearity is repeatable, many dataloggers can be programmed to convert resistance to temperature using the Steinhart–Hart or  $\beta$ -parameter equation.

These equations are not difficult to implement in software (e.g., spreadsheet) if the datalogger is not programmable. Also, thermistor and/or bridge resistor combinations that yield a more linear relationship between resistance and temperature are available and have been used in meteorological measurement networks (less commonly used now because of increased measurement resolution and processing capability of data acquisition systems).

Platinum resistance thermometers have the reputation of being very stable over time, but the platinum sensing element is relatively fragile when compared to a thermistor. Shift or drift in the resistance to temperature relationship of a PRT can be caused by thermal cycling or mechanical shock displacing the sensing element.

Historically, thermistors have been considered less stable than PRTs, but encasing thermistors in an epoxy or glass housing to keep moisture away from the sensing element gives them stability similar to PRTs. When exposed, oxidation of the sensing element can occur, leading to drift in the resistance to temperature relationship of the thermistor. Thermistors sealed in weatherproof housings can be very stable when measurements are made at environmental temperatures. Twelve replicate 2-mm diam. thermistors in epoxy housings (Measurement Specialties model 10K3A11A) were thermal cycled 96 times from -20 to 60 °C, with a corresponding vapor pressure range of 0.5 to 12 kPa, in a test chamber. The thermistors were stable within 0.015 °C (Fig. 3), which is within the uncertainty range of the experiment. A second group of twelve replicates of the same model of thermistor were thermal cycled (same conditions as the initial group) 584 times. Temperature measurements were only made at the beginning and end of thermal cycling. None of the thermistors drifted by more than 0.015 °C. Nine replicates of the same model of thermistors were also deployed in radiation shields outdoors in Logan, Utah (UT), United States, for over two years and no detectable drift was measured.

Response time for air temperature sensors is important for applications where high frequency data are required, and can be critical for accurate measurements of minimum and maximum temperatures. Air temperature measurements from electronic sensors are typically made at relatively high frequencies (every few seconds), but they are often averaged over longer time intervals (every few minutes). Response time does not always need to be rapid for temperature measurements averaged over a longer time interval. Response time is a function of thermal mass of the sensor. More thermal mass means longer response times because equilibration with air is slower. Response time of thermocouples can be reduced by decreasing the diameter of the wire, but the tradeoff is a more fragile sample junction. Response times of thermistors and PRTs can be reduced by mounting the resistive element in a smaller casing, as long as it is rugged and weatherproof. Response time is also influenced by exposure and type of shield sensors are housed in (discussed below). Response times are faster in active (fan-ventilated) shields.

Thermocouples, thermistors, and PRTs all have errors caused by heat conduction down the cable to the sensing element. This error has been documented for type-T thermocouples used to measure leaf temperatures (Tarnopolsky and Seginer, 1999), but the concept is the same for air temperature measurements. If the lead cable is exposed to a heat source, such as solar radiation, it warms and heat is conducted to the sensing element. Heat conduction can be reduced by building and/or using sensors with wire material that has low thermal conductivity. For example, the thermal conductivity of copper is  $386 \text{ W m}^{-1} \text{ K}^{-1}$ , whereas thermal conductivity for chromel and constantan (two common metals used in thermocouples) is about twenty times less at  $19$  and  $21 \text{ W m}^{-1} \text{ K}^{-1}$ , respectively. For this reason, copper wire should be avoided in air temperature sensors. Heat conduction can also be reduced by shielding cables from direct radiation (e.g., cables are often mounted on the bottom of cross-arms on weather stations to reduce absorption of solar radiation).

### Integrated Circuit Sensors

An integrated circuit (IC) temperature sensor is a semiconductor component integrated into a circuit board. Signal (current or voltage) from the semiconductor is temperature dependent, and can be related to absolute temperature. Many circuit boards have IC sensors onboard, but their use as air temperature sensors has not been widespread. Accuracy specifications for IC temperature sensors are typically lower than other sensors (some new IC sensors have accuracy specifications similar to traditional temperature sensors). Also, circuit boards generate heat, which can influence the temperature of components on the board, including IC temperature sensors. The advantage of IC temperature sensors is low cost.

### Sonic Thermometers

Sonic anemometers measure the travel time of acoustic signals over a fixed distance. Travel time of an acoustic signal is linearly dependent on the wind velocity component along the distance traveled. Sonic anemometers have been used for decades to measure wind speed, especially in micrometeorological studies (Kaimal and Businger, 1963; Mitsuta, 1966; Schotland, 1955; Suomi, 1957).

The speed of sound in air ( $c$ ) is dependent on air temperature ( $T$ , in units of K):

$$c^2 = \gamma R_{\text{specific}} T (1 + 0.32 \chi_w) \quad [10]$$

where  $\gamma$  is the heat capacity ratio for air (ratio of heat capacity at constant pressure to heat capacity at constant volume, 1.4 for dry air at 20 °C),  $R_{\text{specific}}$  is the specific gas constant for air (universal gas constant divided by the molar mass of air, 287 J kg<sup>-1</sup> K<sup>-1</sup>), and  $\chi_w$  is the water vapor mole fraction (ratio of moles of water vapor in air to moles of air, in units of mol mol<sup>-1</sup>). Water vapor increases the speed of sound in air and the term  $(1 + 0.32\chi_w)$  accounts for this effect. Rearrangement of Eq. [10] to solve for  $T$  provides a measurement of air temperature from sonic measurement of  $c$  and measurement of humidity ( $\chi_w$ ). Thus, a sonic anemometer can serve as a sonic thermometer if a humidity measurement is available. A sonic thermometer is directly connected to first principles because the speed of sound in a gas (air in this case) is directly related to the thermodynamic temperature of the gas. Sonic thermometry has been proposed as a means of measuring air temperature (Barrett and Suomi, 1949; Pardue and Hedrich, 1956), often for micro-meteorological studies (Kaimal and Gaynor, 1991; Schotanus et al., 1983).

The advantage of sonic thermometry is the absence of a physical sensor (thermal mass) that must equilibrate with air. This provides rapid response time and eliminates radiant heating of the sensor. This means temperature derived from sonic measurements can be used as a reference to determine the influence of radiant heating on physical sensors (discussed below). The disadvantages of sonic thermometry are the high cost and high power requirements of sonic anemometers, and requirement of a humidity measurement and correction. The humidity term  $(1 + 0.32\chi_w)$  is in the denominator when Eq. [10] is rearranged to solve for temperature, so the temperature measurement is high if  $\chi_w$  is low and low if  $\chi_w$  is high. At a  $\chi_w$  value of 15 mmol mol<sup>-1</sup> (characteristic of the semiarid climate of Logan, UT, in summer months), an error of 10% in  $\chi_w$  causes an error of 0.14 °C in air temperature. At a  $\chi_w$  value of 5 mmol mol<sup>-1</sup> (characteristic of the semiarid climate of Logan, UT, in winter months), an error of 10% in  $\chi_w$  causes an error of 0.04 °C. Error scales with  $\chi_w$  thus air temperature errors resulting from inaccurate  $\chi_w$  measurement will be higher for summer months and lower for winter months, and higher for humid places and lower for arid places. Absolute accuracy of measurement of the speed of sound in air ( $c$ ) also affects the temperature measurement. Inaccuracy of the sonic anemometer can result from small changes in sonic sensor spacing with temperature, sensor drift with temperature, and distortion from strong cross wind.

### Housing Air Temperature Sensors

The challenge of accurate air temperature measurement is far greater than having an accurate sensor, as sensors must be in thermal equilibrium with air. Housings for sensors should minimize heat gains and losses due to conduction and radiation, enhance coupling to air via convective currents, and protect sensors from snow and ice accumulation. Radiation-induced heating increases as wind speed (convection) decreases and as radiation load increases (Fig. 4; Bugbee et al., 1996). The housing for an air temperature sensor must shield it from shortwave (solar) radiant heating and longwave radiant cooling. A temperature sensor should also be thermally isolated from the housing to minimize heat transport to and

from the sensor by conduction. The housing should provide ventilation so the temperature sensor is in thermal equilibrium with the air. In addition, the housing should keep precipitation off the sensor, as precipitation causes evaporative cooling. Conversely, condensation on sensors causes warming, and when condensed water subsequently evaporates it cools the sensor.

Radiation shields for air temperature sensors should be in a location with representative air temperature (tops of buildings and areas where they will be influenced by reflection of solar radiation should be avoided). Conditions in microenvironments have the potential to be very different from surrounding conditions. Typical mounting heights for air temperature sensors are 1.2 to 2.0 m above the ground. Radiation shields should be mounted over vegetation.

Temperature sensors on automated weather stations are typically shielded from solar radiation by either a passive (naturally-ventilated) or an active (fan-ventilated) housing (Fig. 5). Passive radiation shields are louvered enclosures that rely on natural ventilation from wind to dissipate absorbed solar energy and equilibrate the sensor to air. Active radiation shields dissipate absorbed solar energy and maintain equilibrium with air through fan ventilation.

### Passive Shields

Passive shields are simple, low-cost, and do not require power, but they warm above air temperature in low wind or high solar radiation (Fig. 6). Warming is increased when there is snow on the ground due to higher albedo and increased reflected solar radiation (Nakamura and Mahrt, 2005), resulting in more incident radiation from below. Errors as high as 10 °C have been reported in passive shields over snow (Genthon et al., 2011; Huwald et al., 2009). Warming is also increased when the sun is low in

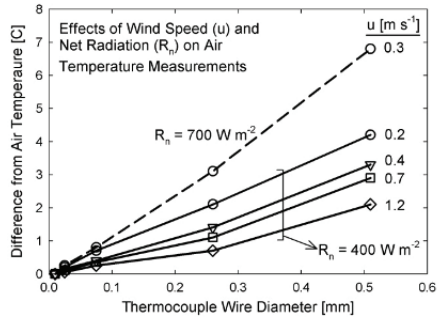


**Fig. 4.** Effects of wind speed ( $u$ ) ( $\text{m s}^{-1}$ ) and net radiation ( $R_n$ ) ( $\text{W m}^{-2}$ ) on air temperature measurements from unshielded type-E thermocouples as a function of thermocouple wire diameter (mm). The wire diameters from smallest to largest are 56-AWG (0.01 mm), 50-AWG (0.03 mm), 40-AWG (0.08 mm), 30-AWG (0.25 mm), and 24-AWG (0.51 mm). Difference from air temperature (y axis) is error of each thermocouple relative to actual air temperature. Data points represent the mean of three thermocouples (standard deviation was smaller than symbol size). Dashed line is the difference for greater  $R_n$  ( $700 \text{ W m}^{-2}$ ), indicating the difference from air temperature is proportional to radiation load. At a given  $u$ , temperature difference increases approximately linearly with increasing wire diameter [data from Bugbee et al. (1996)].



**Fig. 5.** Passive (left) and active (right) radiation shields. Both models (R. M. Young 41003 and R. M. Young 43502) are shown only as examples. Multiple models of passive and active shields are available from several manufacturers.

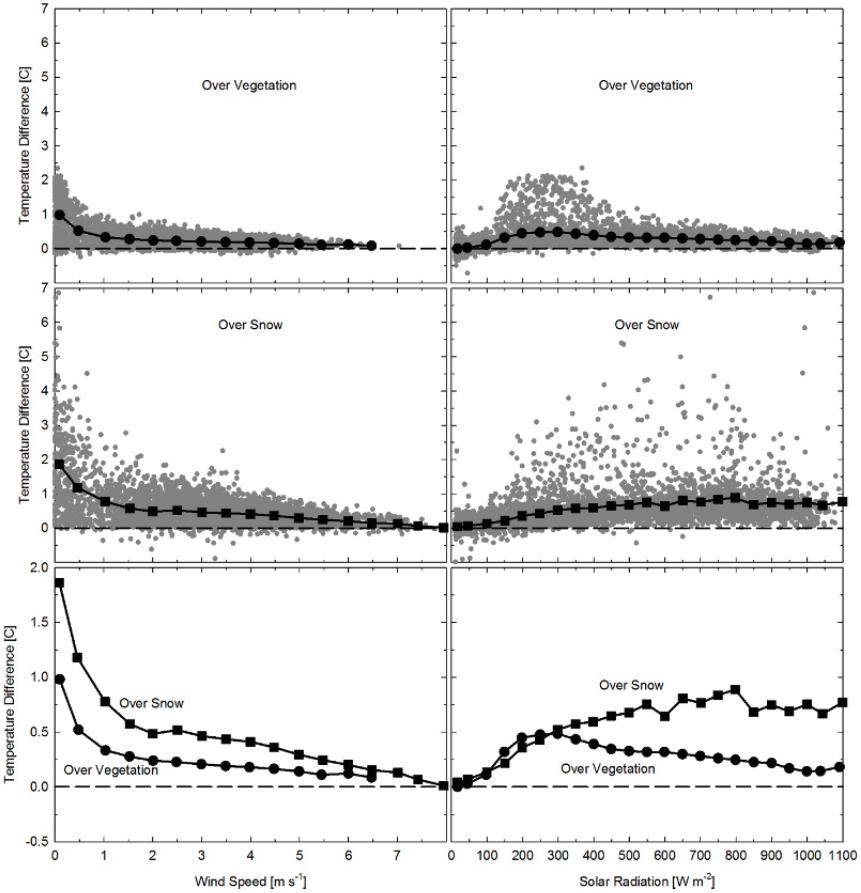


**Fig. 6.** Difference in air temperature measurements between a passive (6-plate, R. M. Young model 41303) and active (Apogee Instruments model TS-100) shield housing identical air temperature sensors (small thermistor, Apogee Instruments model ST-110). Top graph is daytime data collected over vegetation (no snow on the ground) and middle graph is daytime data collected over snow. Black lines are bin averages, and bottom graph shows a comparison of bin averages for conditions of no snow and snow (note y axis scale range is reduced to clearly show differences). Graphs on left hand side are differences with wind speed and graphs on right hand side are differences with solar radiation.

the sky (high solar zenith angles) because more radiation reaches the air temperature sensor through the open sides of passive shields. This is why temperature differences of a passive shield relative to an active shield over vegetation are often greatest from about 200 to 300  $W m^{-2}$  and decline as solar radiation increases (Fig. 6).

Several models of passive radiation shields are available and not all models perform the same. Comparison of three models (R. M. Young model 41003, MetSpec model RAD 16 Mk 1, MetSpec model RAD 16 Mk 2) indicated mean differences of a few tenths of a degree ( $^{\circ}C$ ) at low wind speed (Fig. 7). Trends are similar for all passive shields, with the largest air temperature errors in conditions

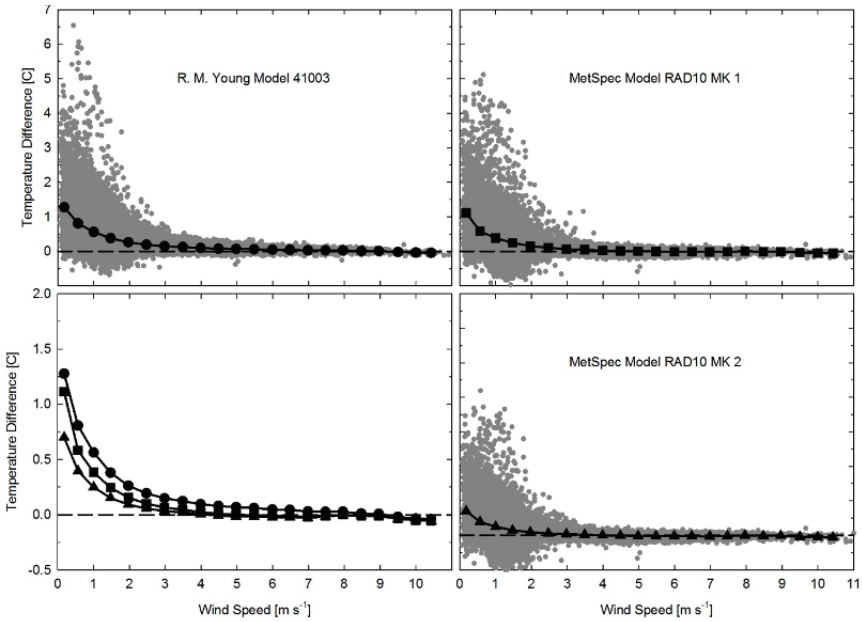
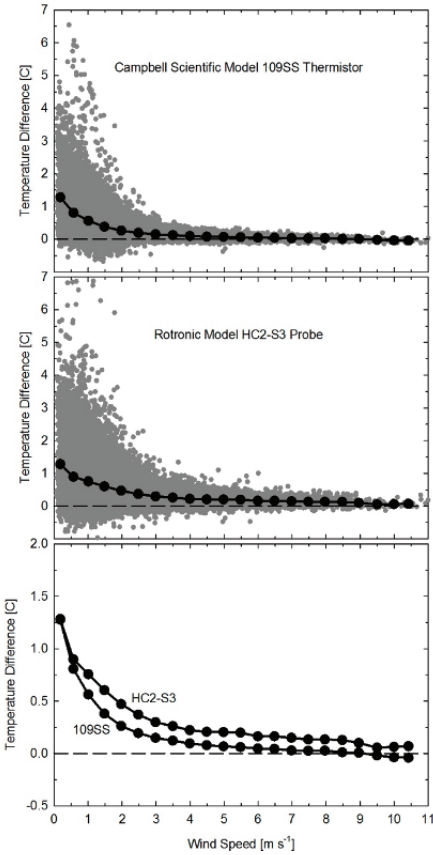


Fig. 7. Difference in air temperature measurements between three models of passive shields (R. M. Young model 41003, MetSpec model RAD10 Mk 1, MetSpec model RAD10 Mk2) and an active shield (Apogee Instruments model TS-100). Air temperature sensors were identical among housings (small thermistor, Campbell Scientific model 109SS). Data were collected over two years and include daytime measurements over vegetation and snow. Black lines are bin averages, and are compared in the graph in the lower left-hand corner (note y axis scale range is reduced to clearly show differences).



Fig. 8. Size comparison of some common temperature and relative humidity probes and two stand-alone temperature sensors (PRT and thermistor). Ruler scale is inches.



**Fig. 9.** Difference in air temperature measurements between two replicates of the same passive shield model (R. M. Young model 41003) and an active shield (Apogee Instruments model TS-100). One of the passive shields housed a small thermistor (Campbell Scientific model 109SS) and the other housed a combined temperature and/or relative humidity probe (Rotronic model HC2-S3). Data were collected over a two year period and include daytime measurements over vegetation and snow. Black lines are bin averages, and are compared in the bottom graph (note y-axis scale range is reduced to clearly show differences).

of high solar zenith angle (morning and evening) and low wind speed. Lopardo et al. (2014) found that errors were larger with older passive radiation shields (by as much as 1.6 °C for a five-year-old shield), presumably because of decreased shortwave reflectivity caused by aging. Temperature sensors in passive shields are better equilibrated to air under high wind speeds. A wind speed of 4 m s<sup>-1</sup> represents an approximate threshold for low albedo (surface reflectivity) conditions over a vegetative surface. At wind speeds greater than about 4 m s<sup>-1</sup>, air temperature measurements in three passive shield models matched measurements from active shields within about 0.1 °C (Fig. 7). Data from Tanner et al. (1996) indicate a wind speed of about 4 m s<sup>-1</sup> is the point where passive shields match active shields. Comparison of passive shields from one weather network to active shields from another weather network revealed passive shields measured warmer daily maximum temperatures (mean was 0.48 °C) and colder daily minimum temperatures (mean was -0.36 °C) (Leeper et al., 2015).

The magnitude of temperature errors caused by radiant heating of sensors in passive shields is highly dependent on the surface area of the sensor. Many weather stations have combined relative humidity and temperature sensors, which are much larger (more surface area) than stand-alone air temperature sensors (Fig. 8). Air temperature errors generally increase with increasing surface area

of the sensor (Fig. 9). Tanner (2001) reported similar results, where a common temperature and/or RH probe (Vaisala model HMP35C) was about 0.5 °C warmer than a medium sized thermistor (Campbell Scientific model 107). Fine-wire thermocouples have been used in passive shields because surface area is minimized (Kurzeja, 2010). Thermal mass of temperature sensors has a major impact on sensor response time. Sensors with small thermal mass equilibrate and respond to

changes quicker and are necessary for applications requiring high frequency air temperature measurements.

Equations to correct air temperature measurements in passive shields have been proposed, but often require measurement of wind speed and solar radiation, and are applicable to specific shield designs (Mauder et al., 2008). Corrections that don't require additional meteorological measurements have also been proposed, such as air temperature adjustment based on the difference between air temperature and interior plate temperature differences (Kurzeja, 2010). Others have suggested modifying traditional multi-plate passive shields to include a small fan that can be operated under specific conditions, but utilize natural aspiration when wind speeds are above an established threshold (Richardson et al., 1999).

### Active Shields

Warming of air temperature sensors above actual air temperature is minimized with active shields, but power is required for the fan. The power requirement for active shields ranges from one to six watts (80–500 mA at 12 V DC). For solar-powered weather stations this can be a major fraction of power usage for the entire station and has typically required a large solar panel and large battery. Power requirement and cost are disadvantages of active shields (Table 3), and they have led to the use of less accurate passive shields on many solar-powered stations. Also, the fan motor can heat air as it passes by the fan. Active shields should be constructed to avoid recirculation of heated air back into the shield.

There is no reference standard for the elimination of radiation-induced temperature increase of a sensor for air temperature measurement, but well-designed active shields minimize this effect. Radiation-induced temperature increase for active shields was analyzed in long-term experiments over snow and grass surfaces by comparing temperature measurements from three models of active radiation shields (Apogee Instruments model TS-100, Met One model 076B, and R. M. Young model 43502). The study included two replicates of each shield model, with matching 2-mm diam. calibrated thermistors in all shields (Apogee Instruments model ST-110). Continuous measurements for two months in summer and two months in winter in Logan, UT, indicated that mean differences among shields were less than 0.1 °C in summer when measurements were made over vegetation, but were as high as 0.4 °C for the R. M. Young shield in winter when measurements were made over snow (Fig. 10). Differences increased with increasing solar radiation, particularly during winter months when there was snow (high reflectivity) on the ground. The Met One model 076B shield was used as a reference because temperatures from this shield tended to be slightly cooler than temperatures from the other two shield models over vegetation.

**Table 3. Advantages and disadvantages of passive (naturally-ventilated) and active (fan-ventilated) radiation shields.**

Shield type	Advantages	Disadvantages
Passive (naturally-ventilated)	Do not require power Lower cost	Less accurate (overheat in low wind or high solar radiation)
Active (fan-ventilated)	More accurate	Require power Higher cost

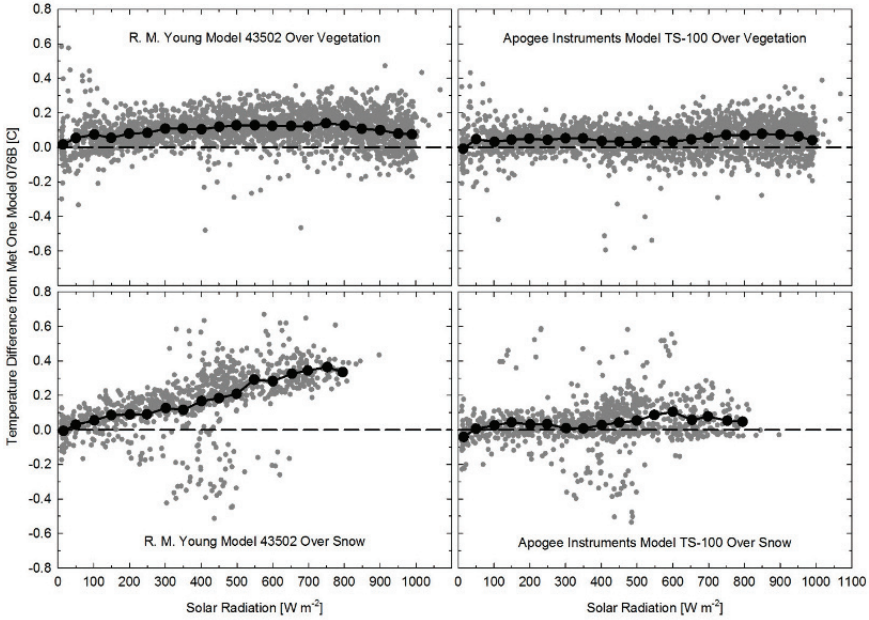


**Fig. 10.** Air temperature differences of two active shields (R. M. Young model 43502, left side, and Apogee Instruments model TS-100, right side) from a reference active shield (Met One model 076B, used as the reference because it tended to measure slightly cooler than the other two models over vegetation). Top graphs are data over vegetation (66 d from summer 2012) and bottom graphs are data over snow (64 d from winter 2013). A small thermistor (Apogee Instruments model ST-110) was used to measure temperature in all shields. All data are from daytime under clear sky conditions and low wind speed (less than 2 m s<sup>-1</sup>). Black lines are bin averages. All sensors were within 0.05 °C at night, indicating minimal differences among sensors.

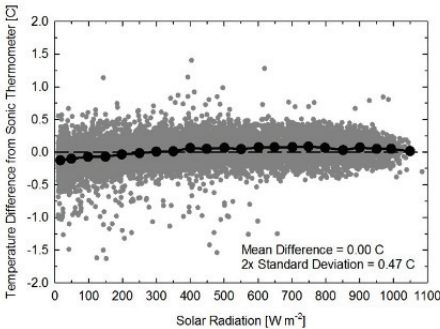


**Fig. 11.** Differences of air temperature measured in an active shield (Apogee Instruments model TS-100 with an Apogee Instruments model ST-110 thermistor) to air temperature from a sonic thermometer (Campbell Scientific model IRGASON). Data are from daytime only and were collected over a one-year period in Logan, Utah (United States). Black line is a bin average.

At higher wind speeds (greater than 3 m s<sup>-1</sup>) during daytime, sensors in the Apogee model TS-100 read slightly cooler on average (-0.05 to -0.1 °C) than sensors in the Met One model 076B and R. M. Young model 43502 shields, possibly due to the ninety degree inlet orifice of the 076B and 43502 shields, which may have reduced the inlet air velocity, and thus ventilation of the thermistor, during high cross winds. Tanner et al. (1996) found passive shields read 0.0 to 0.3 °C cooler than an active shield with a ninety degree inlet at wind speeds greater than about 4 m s<sup>-1</sup>, indicating

poor ventilation of the temperature sensor inside the active shield during higher wind speed.

As mentioned, there is not a reference standard for radiation-induced temperature increase of air temperature sensors, but measurements from sensors in radiation shields can be compared with measurements from sonic thermometry, which does not require equilibration of a physical sensor with the surrounding air. This comparison was done using daytime data from a small thermistor (Apogee Instruments model ST-110) in an active shield (Apogee Instruments model TS-100) and a sonic thermometer (Campbell Scientific model IRGASON, which combines a sonic anemometer and infrared gas analyzer to measure water vapor) over a one-year period in Logan, UT (Fig. 11). Measurements from the active shield were slightly cooler than the sonic thermometer when solar radiation was less than about  $350 \text{ W m}^{-2}$  and slightly warmer when solar radiation was greater than  $350 \text{ W m}^{-2}$ . Average differences were  $0.08 \text{ }^\circ\text{C}$  or less across the range of solar radiation from  $50$  to  $1050 \text{ W m}^{-2}$ . Results were the same when data were analyzed for low wind speeds (less than  $2 \text{ m s}^{-1}$ ). There was a small seasonal dependence of the temperature difference, with the active shield slightly cooler ( $0.09 \text{ }^\circ\text{C}$  on average) than the sonic thermometer in summer and fall and slightly warmer ( $0.09 \text{ }^\circ\text{C}$  on average) than the sonic thermometer in winter and spring. The seasonal dependence appears unrelated to solar radiation intensity, solar zenith angle, and snow on the ground. It is possible the seasonal dependence was related to the humidity measurement that goes into the humidity correction, as the seasonal trend is similar to the trend in water vapor mole fraction ( $\chi_w$ ). The sonic thermometer used for the comparison does not have a specified accuracy, but the close match to the thermistor (accuracy specification of  $\pm 0.1 \text{ }^\circ\text{C}$ ) in the active shield suggests sonic thermometry has potential as a reference for temperature measurements with physical sensors.

### Errors Caused by Rime

Rime can cause large errors in air temperature measurements. Soft rime is relatively common in Logan, UT, on cold, clear winter days when strong air temperature inversions occur. Soft rime is made of tiny ice particles with pockets of air between them, giving it a white color and feathery, needle-like structure. There is relatively poor cohesion between adjacent ice particles, due to rapid freezing of individual super-cooled water droplets when soft rime is formed. This makes soft rime fragile, and easy to remove from surfaces. Soft rime is sometimes called ‘snow feathers’ because of the feathery appearance of the white ice

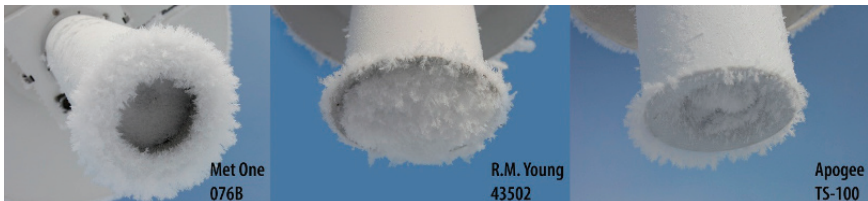


**Fig. 12.** Photo of three models of active shields (Met One 076B, R. M. Young 43502, Apogee Instruments TS-100) with soft rime deposits during a winter temperature inversion in Logan, Utah (United States).

needles and granules that it is composed of. On days when soft rime occurs, the fan on active shields draws it into the shields, sometimes filling the shield (Fig. 12).

Measurements made on days when active shields were full of soft rime indicate Met One model 076B and R. M. Young model 43502 shields tended to read colder than actual air temperature and Apogee model TS-100 shields tended to read warmer than actual air temperature. Actual air temperature was determined by clearing a Met One 076B shield of rime and using the subsequent temperature measurements as the reference. The magnitude of errors appeared to be dependent on the amount of rime inside the shields, with errors of 0.5 to 1.5 °C being typical.

Soft rime also forms on passive shields, but it was difficult to determine temperature errors because soft rime in Logan, UT, occurs on days when passive shield errors are already at a maximum (low wind, clear sky, snow on the ground). However, data indicate passive shield errors were similar to those reported above for conditions of low wind over snow (Fig. 6), independent of whether rime was present or not. Other types of rime and frost would likely have similar impact as soft rime on both active and passive shields. Blowing snow can fill the spaces between the plates on passive shields and significantly reduce ventilation, causing errors similar to those reported for soft rime and detailed above (Fig. 6). Active shields work better in blowing snow as long as snow does not clog the inlet.

## Summary

Accurate air temperature measurement remains challenging, despite decades of research and development to improve instruments and methods. Thermocouples, thermistors, and platinum resistance thermometers (PRTs) have all been used for air temperature measurement in environmental applications, and each have associated advantages and disadvantages. Platinum resistance thermometers have the reputation as the preferred sensor for air temperature measurement due to high accuracy and stability, but modern glass or epoxy coated thermistors are similarly stable, especially at temperatures below 60 °C. Thermistors have high signal-to-noise ratio, are easy to use and low cost, and have accuracy similar to PRTs. Thermocouples have often been used for research purposes, but are becoming less common for air temperature measurement because of the requirement of accurate measurement of reference temperature (datalogger panel temperature).

Methods for shielding and ventilation of the air temperature sensor can be more important than sensor type. Passive, natural ventilation reduces accuracy in conditions of high solar load or low wind speed. Active, fan ventilation improves accuracy compared to passive shields, but increases the cost and power requirement. Sonic thermometry has the potential to be the most accurate because it does not require equilibration of a physical sensor with air, but requires accurate measurements of speed of sound in air and humidity, and the technology is expensive.

Air temperature measurements are an essential component of weather monitoring and climate research worldwide, and will continue to be challenging given the trade-offs between accuracy, power consumption, and costs of the instrument options.

## Acknowledgments

Thanks to Jobie Carlisle at the Utah Climate Center for providing the data shown in Figure 6, Bart Nef at Campbell Scientific for providing the data shown in Figures 7 and 9, Ivan Bogoev at Campbell Scientific for providing the data shown in Figure 11 and reviewing a draft of the manuscript, and Alan Hinckley at Campbell Scientific for reviewing a

draft of the manuscript. Special thanks to Andrew Sandford at Campbell Scientific Limited for reviewing the manuscript and providing multiple suggestions that significantly improved it.

## References

- Barrett, E.W., and V.E. Suomi. 1949. Preliminary report on temperature measurement by sonic means. *J. Meteorol.* 6:273–276. doi:10.1175/1520-0469(1949)006<0273:PROTMB>2.0.CO;2
- Bugbee, B., O. Monje, and B. Tanner. 1996. Quantifying energy and mass transfer in crop canopies: Sensors for measurement of temperature and air velocity. *Adv. Space Res.* 18:149–156. doi:10.1016/0273-1177(95)00871-B
- Callendar, H.L. 1887. On the practical measurement of temperature: Experiments made at the Cavendish Laboratory, Cambridge. *Philos. Trans. R. Soc. Lond. A* 178:161–230. doi:10.1098/rsta.1887.0006
- Christian, K.A., and C.R. Tracy. 1985. Measuring air temperature in field studies. *J. Therm. Biol.* 10:55–56. doi:10.1016/0306-4565(85)90012-9
- Clark, M.R., D.S. Lee, and T.P. Legg. 2013. A comparison of screen temperature as measured by two Met Office observing systems. *Int. J. Climatol.* 34:2269–2277. doi:10.1002/joc.3836
- Genthon, C., D. Six, V. Favier, M. Lazzara, and L. Keller. 2011. Atmospheric temperature measurement biases on the Antarctic plateau. *J. Atmos. Ocean. Technol.* 28:1598–1605. doi:10.1175/JTECH-D-11-00095.1
- Holden, Z.A., A.E. Klene, R.F. Keefe, and G.G. Moisen. 2013. Design and evaluation of an inexpensive radiation shield for monitoring surface air temperatures. *Agric. For. Meteorol.* 180:281–286. doi:10.1016/j.agrformet.2013.06.011
- Hubbard, K.G., and S.E. Hollinger. 2005. Standard meteorological measurements. In: J.L. Hatfield and J.M. Baker, editors, *Micrometeorology in agricultural systems*. American Society of Agronomy, Madison, Wisconsin. p. 1–30.
- Huwald, H., C.W. Higgins, M.-O. Boldi, E. Bou-Zeid, M. Lehning, and M.B. Parlange. 2009. Albedo effect on radiative errors in air temperature measurements. *Water Resour. Res.* doi:10.1029/2008WR007600
- International Electrotechnical Commission. 2017. IEC 60751:2008. Industrial platinum resistance thermometers and platinum temperature sensors. International Electrotechnical Commission. <https://webstore.iec.ch/publication/3400> (verified 10 Oct. 2017). [2017 is year accessed].
- Kaimal, J.C., and J.A. Businger. 1963. A continuous wave sonic anemometer-thermometer. *J. Appl. Meteorol.* 2:156–164. doi:10.1175/1520-0450(1963)002<0156:ACWSAT>2.0.CO;2
- Kaimal, J.C., and J.E. Gaynor. 1991. Another look at sonic thermometry. *Boundary-Layer Meteorol.* 56:401–410. doi:10.1007/BF00119215
- Kurzeja, R. 2010. Accurate temperature measurements in a naturally-aspirated radiation shield. *Boundary-Layer Meteorol.* 134:181–193. doi:10.1007/s10546-009-9430-2
- Leeper, R.D., J. Rennie, and M.A. Palecki. 2015. Observational perspectives from U.S. Climate Reference Network (USCRN) and Cooperative Observer Program (COOP) Network: Temperature and precipitation comparison. *J. Atmos. Ocean. Technol.* 32:703–721. doi:10.1175/JTECH-D-14-00172.1
- Lopardo, G., F. Bertiglia, S. Curci, G. Roggero, and A. Merlone. 2014. Comparative analysis of the influence of solar radiation screen ageing on temperature measurements by means of weather stations. *Int. J. Climatol.* 34:1297–1310. doi:10.1002/joc.3765
- Mauder, M., R.L. Desjardins, Z. Gao, and R. van Haarlem. 2008. Errors of naturally ventilated air temperature measurements in a spatial observation network. *J. Atmos. Ocean. Technol.* 25:2145–2151. doi:10.1175/2008JTECHA1046.1
- Mitsuta, Y. 1966. Sonic anemometer-thermometer for general use. *J. Meteorol. Soc. Jpn.* 44:12–24. doi:10.2151/jmsj1965.44.1\_12
- Nakamura, R., and L. Mahrt. 2005. Air temperature measurement errors in naturally ventilated radiation shields. *J. Atmos. Ocean. Technol.* 22:1046–1058. doi:10.1175/JTECH1762.1
- Pardue, D.R., and A.L. Hedrich. 1956. Absolute method for sound intensity measurement. *Rev. Sci. Instrum.* 27:631. doi:10.1063/1.1715654

- Richardson, S.J., F.V. Brock, S.R. Semmer, and C. Jirak. 1999. Minimizing errors associated with multiplate radiation shields. *J. Atmos. Ocean. Technol.* 16:1862–1872. doi:10.1175/1520-0426(1999)016<1862:MEAWMR>2.0.CO;2
- Schotanus, P., F.T.M. Nieuwstadt, and H.A.R. De Bruin. 1983. Temperature measurement with a sonic anemometer and its application to heat and moisture fluxes. *Boundary-Layer Meteorol.* 26:81–93. doi:10.1007/BF00164332
- Schotland, R.M. 1955. The measurement of wind velocity by sonic means. *J. Meteorol.* 12:386–390. doi:10.1175/1520-0469(1955)012<0386:TMOWVB>2.0.CO;2
- Steinhart, J.S., and S.R. Hart. 1968. Calibration curves for thermistors. *Deep-Sea Res. and Oceanogr. Abstr.* 15:497–503. doi:10.1016/0011-7471(68)90057-0
- Suomi, V.E. 1957. Energy budget studies and development of the sonic anemometer for spectrum analysis. AFCRC Technical Report 56-274, University of Wisconsin, Department of Meteorology, Madison, WI.
- Tanner, B.D. 2001. Evolution of automated weather station technology through the 1980s and 1990s. In: K.G. Hubbard and M.V.K. Sivakumar, editors, *Automated weather stations for applications in agriculture and water resources management: Current uses and future perspectives*. WMO/TD number 1074. World Meteorological Organization, Geneva, Switzerland. p. 3–20.
- Tanner, B.D., E. Swiatek, and C. Maughan. 1996. Field comparisons of naturally ventilated and aspirated radiation shields for weather station air temperature measurements. *Conference on Agricultural and Forest Meteorology with Symposium on Fire and Forest Meteorology* 22:297–300.
- Tarnopolsky, M., and I. Seginer. 1999. Leaf temperature error from heat conduction along thermocouple wires. *Agric. For. Meteorol.* 93:185–194. doi:10.1016/S0168-1923(98)00123-3
- Thomas, C.K., and A.R. Smoot. 2013. An effective, economic, aspirated radiation shield for air temperature observations and its spatial gradients. *J. Atmos. Ocean. Technol.* 30:526–527. doi:10.1175/JTECH-D-12-00044.1
- Van Dusen, M.S. 1925. Platinum-resistance thermometry at low temperatures. *J. Am. Chem. Soc.* 47:326–332. doi:10.1021/ja01679a007
- Young, D.T., L. Chapman, C.L. Muller, and X.-M. Cai. 2014. A low-cost wireless temperature sensor: Evaluation for use in environmental monitoring applications. *J. Atmos. Ocean. Technol.* 31:938–944. doi:10.1175/JTECH-D-13-00217.1